Published OnlineFirst March 27, 2014; DOI: 10.1158/0008-5472.CAN-13-2470

Molecular and Cellular Pathobiology

Cancer Research

Biallelic *DICER1* Mutations in Sporadic Pleuropulmonary Blastoma

Masafumi Seki[1], Kenichi Yoshida[2,6], Yuichi Shiraishi[3], Teppei Shimamura[3], Yusuke Sato[2,6], Riki Nishimura[1], Yusuke Okuno[2], Kenichi Chiba[3], Hiroko Tanaka[4], Keisuke Kato[7], Motohiro Kato[1,5,8], Ryoji Hanada[5], Yuko Nomura[9], Myoung-Ja Park[10], Toshiaki Ishida[11], Akira Oka[1], Takashi Igarashi[1,12], Satoru Miyano[3,4], Yasuhide Hayashi[9], Seishi Ogawa[2,6], and Junko Takita[1]

Abstract

Pleuropulmonary blastoma (PPB) is a rare pediatric malignancy whose pathogens are poorly understood. Recent reports suggest that germline mutations in the microRNA-processing enzyme DICER1 may contribute to PPB development. To investigate the genetic basis of this cancer, we performed whole-exome sequencing or targeted deep sequencing of multiple cases of PPB. We found biallelic *DICER1* mutations to be very common, more common than *TP53* mutations also found in many tumors. Somatic ribonuclease III (RNase IIIb) domain mutations were identified in all evaluable cases, either in the presence or absence of nonsense/frameshift mutations. Most cases had mutated *DICER1* alleles in the germline with or without an additional somatic mutation in the remaining allele, whereas other cases displayed somatic mutations exclusively where the RNase IIIb domain was invariably affected. Our results highlight the role of RNase IIIb domain mutations in *DICER1* along with TP53 inactivation in PPB pathogenesis. *Cancer Res; 74(10); 2742–9. ©2014 AACR.*

Introduction

Pleuropulmonary blastoma (PPB) is an extremely rare and highly aggressive pulmonary malignancy occurring in early childhood. It is characterized histologically by a primitive blastoma and a malignant mesenchymal stroma in the lung that often shows multidirectional differentiation (1). PPB may be sporadic or hereditary and may also present as a part of a familial tumor syndrome (2) consisting of cystic nephroma and other tumor types, such as ovarian tumor, embryonal rhabdomyosarcoma, and malignant germ cell tumors (2). Recently, germline *DICER1* mutations have been demonstrated in majority of patients with PPB and DICER1 syndrome (2, 3). *DICER1* is a member of the ribonuclease III (RNase III) protein family that is involved in the generation of microRNAs (miRNA), modulating gene expression at the posttranscriptional level (4). The DICER1 protein contains RNase IIIa and RNase IIIb domains, which are considered to dimerize intramolecularly with Mg^{2+}/Mn^{2+} to form the active site of the enzyme (5). In PPB, almost all mutations are reported to be heterozygous frameshift or nonsense mutations of germline origin, suggesting an important role of *DICER1* haploinsufficiency in PPB pathogenesis (2, 3). However, most obligate carriers of *DICER1* mutations and heterozygous *Dicer1*-deficient mice did not develop PPB or other types of tumors, suggesting that *DICER1* haploinsufficiency alone is insufficient for tumor development but requires additional genetic alterations (3, 6). To identify a complete set of genetic alterations underlying PPB pathogenesis, we performed whole-exome sequencing of paired tumor and normal DNA from seven cases with sporadic PPB, of which two cases were analyzed for samples obtained at both initial presentation and relapse. Mutations in *DICER1* and other genes were examined by targeted deep sequencing in 16 samples from 12 sporadic PPB cases, including three analyzed by whole-exome sequencing.

Authors' Affiliations: [1]Department of Pediatrics; [2]Cancer Genomics Project, Graduate School of Medicine; Laboratory of [3]DNA Information Analysis and [4]Sequence Data Analysis, Human Genome Center, Institute of Medical Science; [5]Department of Cell Therapy and Transplantation Medicine, The University of Tokyo, Tokyo; [6]Department of Pathology and Tumor Biology, Graduate School of Medicine, Kyoto University, Kyoto; [7]Division of Pediatric Hematology and Oncology, Ibaraki Children's Hospital, Mito, Ibaraki; [8]Department of Hematology/Oncology, Saitama Children's Medical Center, Saitama, Saitama; [9]Department of Pediatrics, School of Medicine, Fukuoka University, Fukuoka; [10]Gunma Children's Medical Center, Shibukawa, Gunma; [11]Department of Hematology and Oncology, Hyogo Prefectural Kobe Children's Hospital, Kobe, Hyogo; and [12]National Center for Child Health and Development, Tokyo, Japan

Note: Supplementary data for this article are available at Cancer Research Online (http://cancerres.aacrjournals.org/).

Corresponding Authors: Junko Takita, Department of Pediatrics, The University of Tokyo, 7-3-1 Hongo, Bunkyo-ku, Tokyo 113-8655, Japan. Phone: 81-3-3815-5411; Fax: 81-3-3816-4108; E-mail: jtakita-tky@umin.ac.jp; and Seishi Ogawa, Department of Pathology and Tumor Biology, Graduate School of Medicine, Kyoto University, Yoshida-Konoe-cho, Sakyo-ku, Kyoto 606-8501, Japan. Phone: 81-75-753-4300; Fax: 81-75-753-9282; E-mail: sogawa-tky@umin.ac.jp

doi: 10.1158/0008-5472.CAN-13-2470

Materials and Methods

Specimens

Genomic DNA for 11 cases was extracted from fresh-frozen samples stored at −80 °C and obtained approximately 2 to 15 years previously. Paraffin-embedded samples were used as tumor samples for cases 10 (at relapse) and 11 (at diagnosis). These samples were stored for approximately 1 year. For

Published OnlineFirst March 27, 2014; DOI: 10.1158/0008-5472.CAN-13-2470

germline control, DNA was obtained from bone marrow blood, peripheral blood, or bone marrow smears in which absence of tumor cells was pathologically confirmed. Bone marrow smears were used as normal samples for cases 05, 07, 08, and 12. This study was approved by The University of Tokyo Ethics Committee (Tokyo, Japan; approval number 1598), and informed consent was obtained from the parents of all participants.

Whole-exome sequencing

Whole-exome sequencing of primary tumor and matched normal specimens of cases 01, 02, 04, 07, 09, 10, and 12 was performed as previously described (7, 8). Relapsed tumor specimens of cases 01 and 02 were also analyzed. Whole-exome capture was accomplished using liquid-phase hybridization of sonicated genomic DNA having a 150 to 200-bp mean length to a bait cRNA library synthesized on magnetic beads (SureSelect Human All Exon Kit V3 or V5, Agilent Technology) according to the manufacturer's protocol. The captured targets were subjected to sequencing using HiSeq 2000 (Illumina) according to the manufacturer's instructions. Raw sequence data were processed using Genomon-exome (http://genomon.hgc.jp/exome/en/index.html) for detection of cancer exome sequencing data through the in-house pipeline constructed at the Human Genome Center, the Institute of Medical Science, The University of Tokyo. Analyses using Genomon are summarized in Supplementary Fig. S1. Sequence data have been deposited at the European Genome-phenome Archive (EGA, http://www.ebi.ac.uk/ega/), which is hosted by the European Bioinformatics Institute, under accession number EGAS00001000662.

Deep sequencing for validation of variants detected by whole-exome sequencing

To validate the mutations detected by whole-exome sequencing, deep sequencing was performed using pair or trio DNA specimens (primary/relapse tumor and normal) using HiSeq 2000 or MiSeq (Illumina). Primers used for this validation are listed in Supplementary Table S1. Mutations were amplified using PCR with a *Not*I linker individually attached to each primer and pooled together on a per-sample basis after successful amplification was confirmed by gel electrophoresis. Pooling was followed by purification of DNA using the FastGene Gel/PCR Extraction Kit (Nippon Genetics) and digestion with *Not*I. The digested DNA was purified again, and an aliquot of purified DNA was ligated with T4 DNA ligase for 5 hours, sonicated into approximately 200 bp fragments on an average using Covaris (Covaris), and used for generation of sequencing libraries with the NEBNext Ultra DNA Library Prep Kit for Illumina (New England Biolabs) according to the manufacturer's protocol. Data processing was performed according to previously described methods (7, 8). Each single-nucleotide variant and each insertion/deletion (indel) whose variant allele frequency (VAF) in the tumor sample was equal to or more than 2.0% and in the germline sample less than 2.0% were assigned as a somatic mutation. If the mutant allele frequency in the matched nontumor sample was more than 2.0%, the mutation was discarded (8). The mutation was evaluated for pathogenicity using the online mutation predicting tool, Mutation Taster (http://www.mutationtaster.org).

Small RNA sequencing

RNA was extracted using the miRNeasy Kit (Qiagen). Total RNA was quantified and evaluated for quality using a bioanalyzer (Agilent Technology). Libraries for small RNA sequencing were generated using the TruSeq small RNA Sample Preparation Kit (Illumina) and analyzed using the Illumina MiSeq according to the manufacturer's protocol. Small RNA sequencing was performed for four cases (cases 01, 07, 08, and 09). Read sequences were aligned against miRBase (release 16) using MiSeq Reporter v2.3 (Illumina). After alignment, the number of read sequences aligned to each miRNA or pre-miRNA was calculated. Gurtan and colleagues demonstrated that the RNase IIIA and IIIB domains of DICER1 process the 3′ (3p) and 5′ (5p) arms of miRNAs, respectively, *in vivo* (9). We defined the pre-miRNA cleavage ratio as the read counts of miRNA/(read counts of pre-miRNA + miRNA). This ratio was calculated for 5p or 3p miRNA, and then compared tumor specimens with fetal lung as normal control. Statistical differences were calculated by Wilcoxon rank-sum test.

Single-nucleotide polymorphism genotyping microarray

DNA of 11 cases (excluding case 11) as well as that of three relapse cases was hybridized to Affymetrix GeneChip 250K Nsp arrays (Affymetrix). DNA of cases 10 (at relapse) and 11 was not hybridized because of the poor quality of DNA from the paraffin-embedded samples. After appropriate normalization of mean array intensities, signal ratios between tumors and anonymous normal references were calculated in an allele-specific manner, and allele-specific copy numbers were inferred from the observed signal ratios based on a hidden Markov model using CNAG software (http://www.genome.umin.jp).

Sanger sequencing and targeted deep amplicon sequencing

Sanger sequencing of *DICER1* and *TP53* was performed for samples from all cases and relapsed tumor samples from four cases. Germline DNA was sequenced for nine cases (including case 02 without *DICER1* mutation). Sanger sequencing of *PDCD2L* and *UBA2* was performed for 11 cases. Deep amplicon sequencing of target exons of *TP53*, *GPR182*, and *CTNNB1* was performed for 14 samples from 11 cases. Exons harboring mutations in *DICER1* were sequenced for 11 cases, and all coding exons of *DICER1* were sequenced for case 02. Details of deep sequencing have been provided above. All primer sequences for these genes are listed in Supplementary Table S2–S4.

Results

The mean coverage in the whole-exome sequencing of tumor and germline samples was 126× and 128× for the 50 Mb target regions, respectively. More than 93% of the coding sequences were represented by more than 20 independent reads on an average (Supplementary Fig. S2). GC content and mean coverage are shown in Supplementary Fig. S3. Mean coverage of high-GC (≥60%) exons was lower than that of low GC (<60%). In total, 217 nonsilent substitutions and 12 indels

Published OnlineFirst March 27, 2014; DOI: 10.1158/0008-5472.CAN-13-2470

were detected across nine tumor specimens, of which 191 (88%) and 12 (100%), respectively, were successfully confirmed by deep sequencing (Supplementary Table S5). The number of nonsilent mutations per sample at presentation (13–35 mutations) was lower than that reported in most solid tumors in adults (10–12), but comparable with the number reported for other pediatric tumors such as neuroblastoma and medulloblastoma (18 and 16, respectively; Fig. 1A; refs. 13, 14). In two cases for which serial samples could be analyzed, relapsed samples had higher mutation number than corresponding samples at initial presentation (Fig. 1A and B). In both cases, intratumoral subpopulations were evident at the time of initial presentation (Fig. 1C). As previously reported for other cancers (15, 16), the clonal architecture of tumor subpopulations underwent dynamic evolutionary alterations during tumor progression. Serial samples in each case had several clonal mutations in common as well as harbored private subclonal mutations of their own (Fig. 1B and C). In case 01, some of the subclonal mutations (purple) found in the initial sample disappeared at relapse and were replaced by new mutations carried by new subpopulations (red), whereas most of the mutations found in the subclones (green) were retained at similar relative allele frequencies in the relapse sample in case 02. In both cases, relapsed tumors were accompanied by newly acquired gene mutations in each subpopulation and/or by appearance of new subclones that were totally absent from the original initial samples (Fig. 1C).

DICER1 mutations were detected for six cases (cases 01, 04, 07, 09, 10, and 12) but not for case 02; targeted deep sequencing was unable to detect any *DICER1* mutations. *DICER1* mutations were found in the major tumor populations in these six cases (Fig. 1C and D). In contrast with previous reports where all *DICER1* mutations were heterozygous and had germline origin, we identified two homozygous somatic *DICER1* mutations in cases 09 and 10, prompting us to investigate the status of *DICER1* mutations in five additional cases. *DICER1* mutations were found in 11 of 12 (92%) cases (Table 1; Fig. 2A and Supplementary Fig. S4), in which six of the 11 cases with *DICER1* mutations carried compound heterozygous mutations. Two cases carried homozygous *DICER1* mutations (Fig. 2B), presumably caused by copy number-neutral LOH (or uniparental disomy; UPD) involving the 14q arm harboring the *DICER1* locus. In total, biallelic *DICER1* mutations were found in eight of the 11 (73%) cases with *DICER1* mutations. We failed to demonstrate biallelic alterations in three cases (case 01, 05, and 11; Table 1 and Supplementary Fig. S4). We confirmed the same *DICER1* mutation status in initial and relapse samples in all four cases, for which both serial samples were available, indicating that *DICER1* mutations are involved in tumor development rather than progression.

Germline DNA was available in eight cases to confirm germline/somatic origins of *DICER1* mutations, of which four (cases 04, 07, 08, and 12) were compound heterozygous for a germline nonsense/frameshift and a somatic missense mutation, two (cases 09 and 10) were homozygous for somatic, missense mutations caused by an acquired UPD, and the remaining cases were heterozygous for a somatic missense mutation (case 01) or a germline frameshift mutation (case 05;

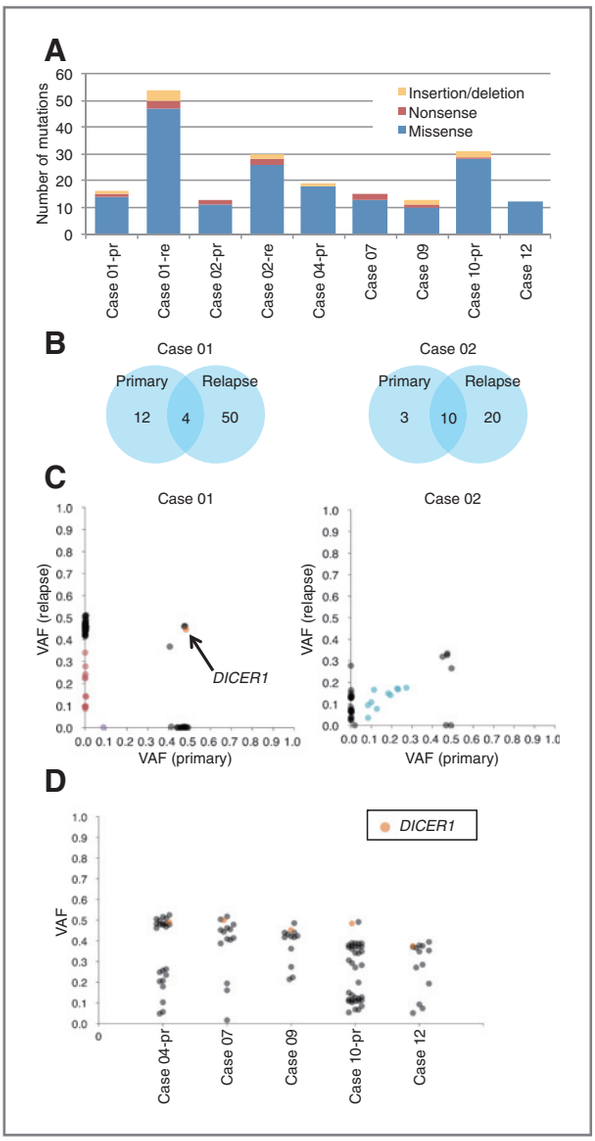

Figure 1. Mutations and mutant allele frequencies detected by whole-exome sequencing in 7 PPB cases. A, type and number of somatic mutations in each tumor. Each mutation type is distinguished using the indicated color. Primary (pr) and relapsed (re) tumors of cases 01 and 02 were examined independently by whole-exome sequencing. B, Venn diagram of somatic mutations found in cases 01 and 02. Both relapsed (re) tumors had increased number of somatic mutations compared with primary (pr) tumors. C, VAF distribution of validated mutations in relapsed cases. VAF was obtained from deep sequencing. Allele frequencies were corrected for copy numbers determined by SNP array analysis. *DICER1* mutation is discriminated by the indicated color in case 01. Case 02 harbored no *DICER1* mutation. Subclonal mutations in case 01 at primary (pr) and relapse (re) are distinguished by purple and red, respectively. Subclonal mutations in case 02 are distinguished by green. D, VAF distribution of validated mutations in nonrelapsed cases. *DICER1* mutations were included in the major tumor population.

Table 1). Among the three cases without normal samples, the combination of a nonsense and missense mutation was also found in the two cases with compound heterozygous mutations. In these cases, a somatic origin was suspected for a

Published OnlineFirst March 27, 2014; DOI: 10.1158/0008-5472.CAN-13-2470

Table 1. Mutations in *DICER1* and *TP53* in sporadic PPB cases

	DICER1				*TP53*				
Case	**Exon**	**Mutation**	**AA change**	**Origin**	**Exon**	**Mutation**	**AA change**	**17p**	**Sample**
01	25	5428G>T	D1810Y	Somatic		Native		Loss	Pr/Re
02		Native				Native			Pr/Re
03	23	4910C>A	S1637X	ND	4	c.332_333delTG	p.L111fs	Loss	Pr
	24	5114A>T	E1705V	ND					
04	21	3482delC	P1161fs	Germline	5	c.527G>T[a]	p.C176F	Loss	Pr/Re
	24	5125G>A	D1709N	Somatic	4	c.313G>A[b]	p.G105S		
05	9	1383delAAAG	I461fs	Germline		Native			Pr
06	19	3007C>T	R1003X	ND		Native			Pr
	25	5428G>T	D1810Y	Probably somatic					
07	18	2863insA	T955fs	Germline	8	c.891_903	p.H297fs	Loss	Pr
	25	5425G>A	G1809R	Somatic		delCGAGCTGCCCCCA			
08	21	3748delC	S1250fs	Germline	7	c.762_764delACAT	p.I254fs	Loss	Pr
	25	5425G>A	G1809R	Somatic					
09	25	5425G>A (Homozygous)	G1809R	Somatic		Native		Loss	Pr
10	25	5425G>A (Homozygous)	G1809R	Somatic	8	c.817C>T	p.R273C	Loss	Pr/Re
11	8	1148dupAGGGT	I383fs	ND		Native		ND	Pr
12	25	5460C>G	Y1820X	Germline		Native		Loss	Pr
	25	5438A>G	E1813G	Somatic					

Abbreviations: ND, not determined; AA, amino acid; Pr, primary; Re, relapse.
[a]Primary tumor.
[b]Relapse tumor.

missense mutation (D1810Y) in case 06, in that the VAF of that mutant deviated significantly from the expected value (0.5) for germline variants (Supplementary Table S6). Conspicuously, all the nine missense *DICER1* mutations found in our cohort were located within the RNase IIIb domain with a mutational hotspot at G1809 (Fig. 2C), for which a somatic origin was confirmed or highly suspected in eight mutations. Combined with previous reports for PPB (2, 3), this high frequency of germline mutations supported the incomplete penetrance of *DICER1* mutations in both familial and sporadic PPB. To assess the effect of *DICER1* mutation in RNase IIIb domain on RNA cleavage, we performed small RNA sequencing in tumors with mutational hotspots at G1809R and D1810Y. Total RNA including miRNA extracted from fetal lung was used as a normal control. Given that the RNase IIIA and IIIB domains of DICER1 process the 3p and 5p arms of miRNAs, respectively (9), *DICER1* mutations in RNase IIIb domain are expected to affect 5p rather than 3p miRNA expression. Comparing the pre-miRNA cleavage ratio of tumor samples to that of the fetal lung control, we confirmed dramatically reduced 5p miRNA expression in the tumors with G1809R and D1810Y mutations ($P < 7.1 \times 10^{-7}$; Fig. 3A and B). In contrast, 3p miRNA expression was significantly higher in the tumor samples than in fetal lung control ($P < 1.4 \times 10^{-3}$), suggesting that G1809R and D1810Y mutants have opposite effects on 3p miRNA cleavage. Taken together, our results suggest that a mutational hotspot at G1809R has a pathogenic effect.

Except for *DICER1*, several genes were found to be recurrently mutated in whole-exome sequencing, including *TP53*, *CTNNB1*, *GPR182*, *MYH8*, *PDE2A*, and *TMX3* (Supplementary Table S7). *TP53*, *CTNNB1*, and *GPR182* were investigated by targeted deep sequencing in an additional five cases, although these genes were not mutated in *CTNNB1* and *GPR182*. The result of targeted deep sequencing in *TP53* is described below. To identify additional genetic alterations, we next performed single-nucleotide polymorphism (SNP) array-based genome-wide copy number analysis in 14 samples of 11 cases for which high-quality genomic DNA was available (including three cases with both primary and relapsed tumors). Chromosome 8q gain was the most common copy number change and was found in 10 of the 11 cases in varying combinations with other genetic changes, including loss of chromosomes 10 and 17p and high-grade amplification of 19q (Fig. 4A and Supplementary Figs. S4 and S5). Chromosome 17p LOH was found in 10 samples and was caused by UPD ($N = 1$) or deletions ($N = 9$), and commonly involved an 8.5-Mb region that contained *TP53*. To investigate a possible role of *TP53* mutations in PPB, we analyzed the *TP53* mutation status in 14 tumor samples from all 12 cases by Sanger and deep sequencing. We detected recurrent missense or frame shift mutations in five of the 12 cases (42%; Fig. 4B; Table 1), in which all five cases were accompanied by 17p LOH and led to biallelic *TP53* inactivation. Intriguingly, in case 04, the relapsed tumor had a different *TP53* mutation (G105S) from that found at the time of initial presentation (C176F), suggesting that the relapse originated from a different subclone in which the two *DICER1* mutations predated *TP53* mutations. We also found several focal amplifications involving 5q23, 6q16-21, 15q23-24, and 19q13.11. However, none of

Published OnlineFirst March 27, 2014; DOI: 10.1158/0008-5472.CAN-13-2470

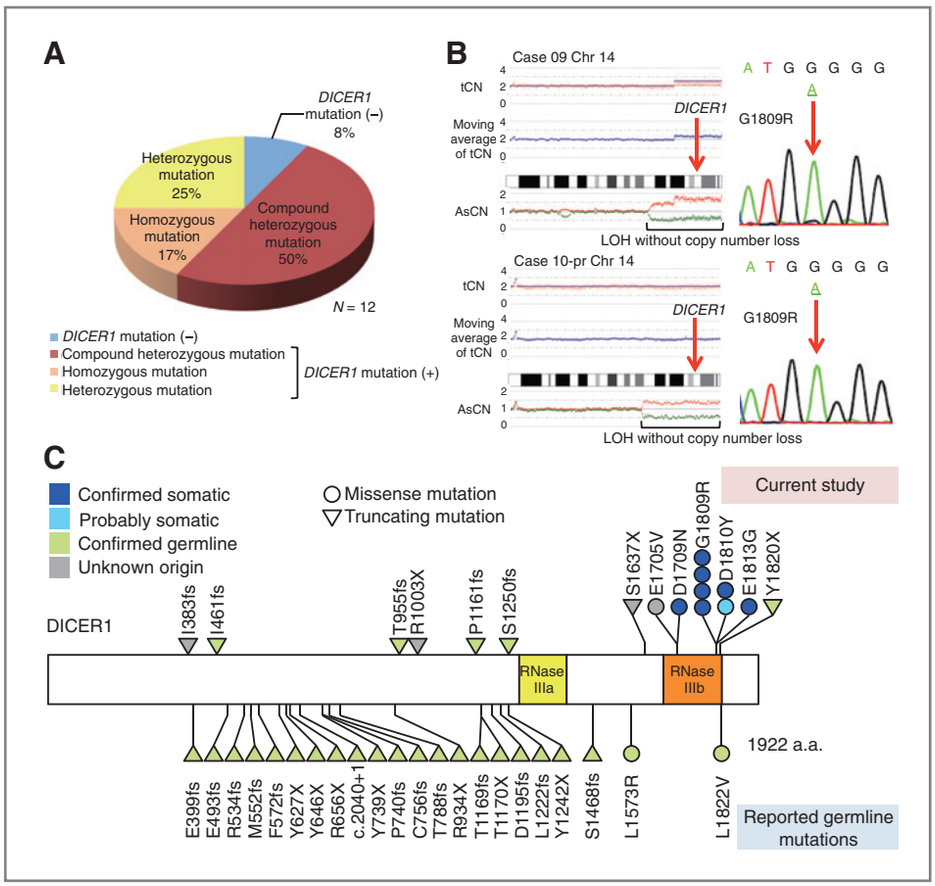

Figure 2. DICER1 abnormalities detected in 12 PPB cases. A, frequency of identified *DICER1* mutations in 12 cases. B, homozygous *DICER1* mutation with 14q LOH without copy number loss. Right panels show a sequence chromatogram of a G1809R homozygous mutation. Left panels show 14q LOH obtained from SNP array analysis. tCN, total copy number; AsCN, allele-specific copy number. C, a schematic of DICER1 protein structure with the positions of alterations. Top and bottom portions indicate mutations detected in our study and previously reported mutations in references 2 and 3, respectively. All the nine missense *DICER1* mutations found in our cohort were located within the RNase IIIb domain with a mutational hotspot at G1809. fs, frameshift.

these amplifications were recurrent, except for those involving 19q13.11, which were found in three (25%) of the 12 cases (Supplementary Fig. S5). The amplified region contains five genes, including *LSM14A*, *KIAA0355*, *GPI*, *UBA2*, and *PDCD2L*, but mutations were detected in none of these genes.

Discussion

The most striking discovery in the present study is the frequent biallelic involvement of *DICER1* mutations in majority of PPB cases with an obligatory missense mutation involving the RNase IIIb domain. In our cohort, biallelic *DICER1* mutations were documented in eight of the 11 *DICER1*-mutated cases with sporadic PBB, with RNase IIIb domain-involving mutations found in all cases and somatic origins demonstrated in all evaluable cases. This result was in stark contrast with previous reports, where all *DICER1* mutations in PPB or *DICER1* syndrome cases were heterozygous and inherited from parents; all mutations were either nonsense or frameshift changes except for two cases, of which one had a missense mutation in the RNase III domain (2, 3). Interestingly, a recent study reported frequent recurrent *DICER1* mutations affecting the RNase IIIb domain in nonepithelial ovarian cancers, especially Sertoli–Leydig cell tumor, in which 26 of 43 tumors carried exclusively RNase IIIb domain mutations with only four tumors being compound heterozygotes of a germline nonsense/frameshift mutation and an RNase IIIb domain mutation (5). Conspicuously, no germline mutations involving the RNase IIIb domain and no biallelic nonsense or frameshift mutations have been reported in any human cancers, possibly accounting for the different spectrum of *DICER1* mutations between PPB and ovarian cancers. These unique features of *DICER1* mutations suggest distinct oncogenic roles of both nonsense/frameshift and RNase IIIb domain mutations. It could be hypothesized that complete loss of DICER1 functions caused by biallelic nonsense/frameshift mutations is not compatible with cell viability, whereas further loss of particular DICER function, beyond haploinsufficiency through targeted mutations within the RNase IIIb domain, could be required or effective for the tumor cells to be clonally selected.

The RNase IIIb domain in DICER1 and other RNase III protein family members is involved in excision of double-stranded miRNA stems, which are then cleaved to single-stranded miRNA through the activity of the RNase IIIa domain (5). A mutation of the conserved amino acids in the RNase IIIb domain could thus lead to compromised miRNA processing, especially in excision of miRNAs. In fact, four mutational hotspots at metal-binding sites (E1705, D1709, D1810, and E1813) found in nonepithelial ovarian cancer were shown to have decreased RNase IIIb activity (5). In the current study, we found an additional mutational hotspot within the RNase IIIb domain affecting a highly conserved amino acid position

Published OnlineFirst March 27, 2014; DOI: 10.1158/0008-5472.CAN-13-2470

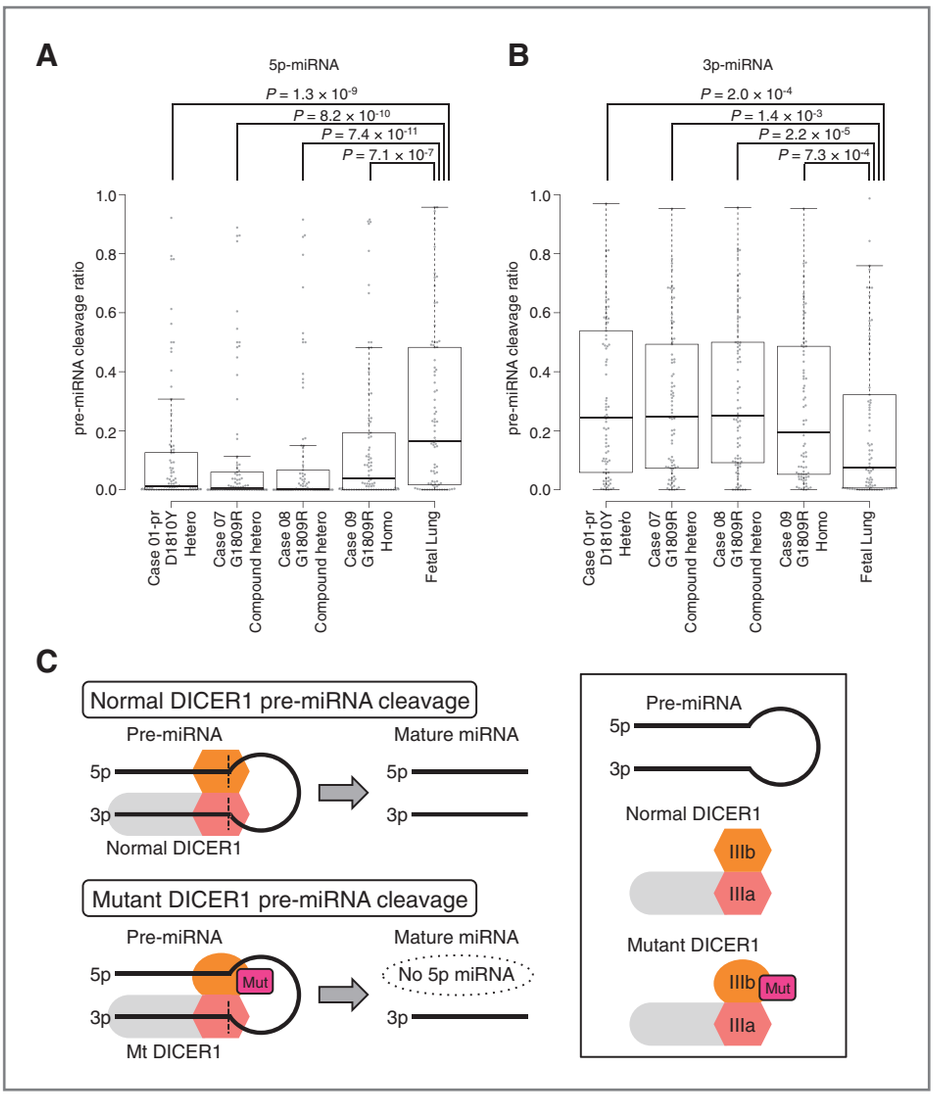

Figure 3. Significant reduction of pre-miRNA cleavage of 5p strand in four tumor specimens by small RNA sequencing. A, 5p miRNA biogenesis was significantly reduced in tumor samples. *P* values were calculated by Wilcoxon rank-sum test. B, 3p miRNA biogenesis was retained in tumor samples. In contrast with 5p miRNA expression, 3p miRNA expression in tumor samples exceeds normal control. C, schematic model of aberrant pre-miRNA cleavage by hotspot mutant DICER1. The miRNA biogenesis pathway by normal DICER1 is indicated in the top panel. A proposed model of hotspot DICER1 mutant is presented in the lower panel. Hotspot DICER1 mutant could not cleave the 5p strand of pre-miRNA. Loss of 5p miRNA may prompt DICER1 to cleave pre-miRNA so that 3p miRNA may be overprocessed.

(G1809) in the vicinity of the two known hotspot codons (D1810 and E1813). Our small RNA sequencing revealed that mutational hotspots at G1809 and a D1810 mutation showed a dramatically reduced cleavage ratio of 5p miRNA, and D1810 mutation also showed the same results in PPB. D1810 mutation is one of the hotspot mutations in nonepithelial ovarian cancer (5), of which reduced 5p miRNA expression has been already confirmed (17). This finding suggests that a specific mutational hotspot of PPB, G1809, is functionally equivalent to hotspot mutations in nonepithelial ovarian cancer. Anglesio and colleagues showed no significant change in 3p miRNA expression (17); however, its cleavage ratio was increased in our analysis. This result may be due to the existence of some mechanism that activates DICER1 to compensate the loss of 5p miRNA production (Fig. 3C). Gurtan and colleagues also mentioned an increased ratio of miRNA star to mature strands relative to cells expressing native hsDicer (9). MiRNA star means less abundant mature miRNA, which usually consists of 3p miRNA, so that this result is compatible with our observation. Thus, it seems that mutations at G1809 could lead to a biologic consequence similar to that of known hotspot mutations (5), although the oncogenic mechanism of the defective cleavage but not excision of miRNAs in the pathogenesis of PPB and other cancers awaits elucidation.

Besides *DICER1* mutations, *TP53* mutations with or without 17p loss as well as trisomy 8 and other chromosomal abnormalities were among the common genetic lesions in PPB. With respect to *DICER1* mutations, it is of note that TP53 also plays a critical role in the regulation of miRNA processing (18). Indeed, tumor-derived transcriptionally inactive TP53 mutants suppress precursor and mature miRNA levels, whereas native TP53 increases them (18), indicating that *TP53* plays an important role in cancer biology via regulation of miRNA processing. A recent study showed that TP53 regulates DICER1 expression via transcriptional miRNAs such as let-7 (19). In contrast, Wang and colleagues showed that knockdown of *DICER1*

Published OnlineFirst March 27, 2014; DOI: 10.1158/0008-5472.CAN-13-2470

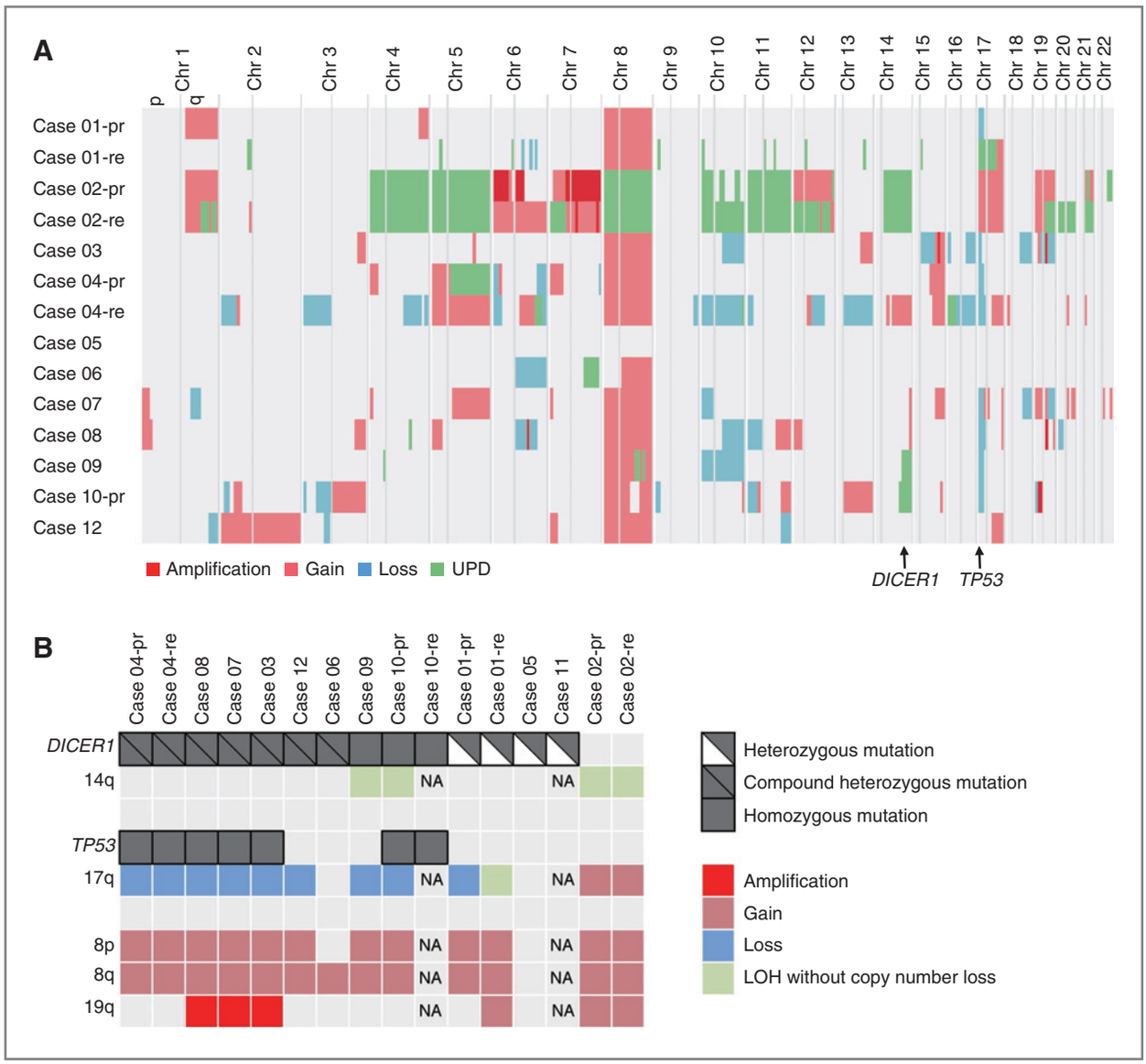

Figure 4. Overview of *DICER1* and *TP53* mutations with copy number alterations. A, copy number alterations by SNP array analysis in 14 PPB samples from 11 cases. The regions of *DICER1* and *TP53* are indicated by arrows. Amplification, gain, loss, and UPD are distinguished by the indicated colors. Copy number (CN) gain was defined as copy number between 3 and 5. Amplification was defined as an inferred copy number of more than 5. Copy number loss was defined as copy number less than one copy and LOH was assigned when one allele was retained. B, distribution of *DICER1* and *TP53* mutations with frequently detected copy number alterations. pr, primary; re, relapse; NA, not available.

expression in BxPC-3 and Panc-1 pancreatic cancer cells resulted in significant increases in TP53 protein levels (20), suggesting the existence of a regulatory loop between TP53, DICER1, and let-7, deregulation of which may play a role in PPB development.

In conclusion, biallelic *DICER1* mutations were common in PPB, invariably accompanied by a somatic RNase IIIb domain mutation. Majority of cases had mutated *DICER1* alleles in germline with or without an additional RNase IIIb domain mutation in the remaining allele. Recurrent mutations were rare in PPB, except for frequent *TP53* deletions/mutations. Our results provide novel insight into the critical role of *DICER1* mutations and importance of *TP53* inactivation in the pathogenesis of PPB.

Disclosure of Potential Conflicts of Interest

No potential conflicts of interest were disclosed.

Authors' Contributions

Conception and design: M. Seki, S. Ogawa, J. Takita
Development of methodology: Y. Shiraishi, Y. Okuno
Acquisition of data (provided animals, acquired and managed patients, provided facilities, etc.): M. Seki, K. Yoshida, Y. Sato, R. Nishimura, Y. Okuno, K. Kato, R. Hanada, Y. Nomura, M.-J. Park, T. Ishida

Published OnlineFirst March 27, 2014; DOI: 10.1158/0008-5472.CAN-13-2470

Analysis and interpretation of data (e.g., statistical analysis, biostatistics, computational analysis): M. Seki, Y. Shiraishi, T. Shimamura, Y. Sato, Y. Okuno, K. Chiba, H. Tanaka, S. Miyano
Writing, review, and/or revision of the manuscript: M. Seki, A. Oka, S. Ogawa, J. Takita
Administrative, technical, or material support (i.e., reporting or organizing data, constructing databases): T. Ishida, Y. Hayashi
Study supervision: T. Igarashi, Y. Hayashi, S. Ogawa, J. Takita

Acknowledgments

The authors thank Matsumura, Hoshino, Yin, Saito, Mori, Nakamura, Mizota, and Drs. K. Ohki and J. Okubo for excellent technical assistance and Drs. Y. Tanaka, K. Ida, A. Motomura, R. Shiozawa, K. Watanabe, and A. Kozaki for assisting with clinical care for patients and collecting samples.

Grant Support

This work was supported by Research on Measures for Intractable Diseases, Health, and Labor Sciences Research Grants, the Ministry of Health, Labour and Welfare; Research on Health Sciences focusing on Drug Innovation; the Japan Health Sciences Foundation, grant from the Ministry of Education, Culture, Sports, Science and Technology of Japan, KAKENHI (22134006), the Project for the Development of Innovative Research on Cancer Therapeutics (P-DIRECT), and also by the Japan Society for the Promotion of Science through the "Funding Program for World-Leading Innovative R&D on Science and Technology (FIRST Program)," initiated by the Council for Science and Technology Policy.

The costs of publication of this article were defrayed in part by the payment of page charges. This article must therefore be hereby marked *advertisement* in accordance with 18 U.S.C. Section 1734 solely to indicate this fact.

Received August 27, 2013; revised February 17, 2014; accepted March 9, 2014; published OnlineFirst March 27, 2014.

References

1. Hill DA, Jarzembowski JA, Priest JR, Williams G, Schoettler P, Dehner LP. Type I pleuropulmonary blastoma: pathology and biology study of 51 cases from the international pleuropulmonary blastoma registry. Am J Surg Pathol 2008;32:282–95.
2. Hill DA, Ivanovich J, Priest JR, Gurnett Ca, Dehner LP, Desruisseau D, et al. DICER1 mutations in familial pleuropulmonary blastoma. Science 2009;325:965.
3. Slade I, Bacchelli C, Davies H, Murray a, Abbaszadeh F, Hanks S, et al. DICER1 syndrome: clarifying the diagnosis, clinical features and management implications of a pleiotropic tumour predisposition syndrome. Am J Med Genet 2011;48:273–8.
4. Carthew RW. Gene regulation by microRNAs. Curr Opin Genet Dev 2006;16:203–8.
5. Heravi-Moussavi A, Anglesio MS, Cheng SW, Senz J, Yang W, Prentice L, et al. Recurrent somatic DICER1 mutations in nonepithelial ovarian cancers. N Engl J Med 2012;366:234–42.
6. Kumar MS, Pester RE, Chen CY, Lane K, Chin C, Lu J, et al. Dicer1 functions as a haploinsufficient tumor suppressor. Genes Dev 2009;23:2700–4.
7. Yoshida K, Sanada M, Shiraishi Y, Nowak D, Nagata Y, Yamamoto R, et al. Frequent pathway mutations of splicing machinery in myelodysplasia. Nature 2011;478:64–9.
8. Yoshida K, Toki T, Okuno Y, Kanezaki R, Shiraishi Y, Sato-Otsubo A, et al. The landscape of somatic mutations in Down syndrome-related myeloid disorders. Nat Genet 2013;45:1293–9.
9. Gurtan AM, Lu V, Bhutkar A, Sharp PA. *In vivo* structure-function analysis of human Dicer reveals directional processing of precursor miRNAs. RNA 2012;18:1116–22.
10. Banerji S, Cibulskis K, Rangel-Escareno C, Brown KK, Carter SL, Frederick AM, et al. Sequence analysis of mutations and translocations across breast cancer subtypes. Nature 2012;486:405–9.
11. Network CGAR. Integrated genomic analyses of ovarian carcinoma. Nature 2011;474:609–15.
12. Network CGAR. Comprehensive genomic characterization of squamous cell lung cancers. Nature 2012;489:519–25.
13. Pugh TJ, Weeraratne SD, Archer TC, Pomeranz Krummel DA, Auclair D, Bochicchio J, et al. Medulloblastoma exome sequencing uncovers subtype-specific somatic mutations. Nature 2012;488:106–10.
14. Pugh TJ, Morozova O, Attiyeh EF, Asgharzadeh S, Wei JS, Auclair D, et al. The genetic landscape of high-risk neuroblastoma. Nat Genet 2013;45:279–84.
15. Ding L, Ley TJ, Larson DE, Miller CA, Koboldt DC, Welch JS, et al. Clonal evolution in relapsed acute myeloid leukaemia revealed by whole-genome sequencing. Nature 2012;481:506–10.
16. Nik-Zainal S, Van Loo P, Wedge DC, Alexandrov LB, Greenman CD, Lau KW, et al. The life history of 21 breast cancers. Cell 2012;149:994–1007.
17. Anglesio MS, Wang Y, Yang W, Senz J, Wan A, Heravi-Moussavi A, et al. Cancer-associated somatic DICER1 hotspot mutations cause defective miRNA processing and reverse-strand expression bias to predominantly mature 3p strands through loss of 5p strand cleavage. J Pathol 2013;229:400–9.
18. Suzuki HI, Yamagata K, Sugimoto K, Iwamoto T, Kato S, Miyazono K. Modulation of microRNA processing by p53. Nature 2009;460:529–33.
19. Lujambio A, Lowe SW. The microcosmos of cancer. Nature 2012;482:347–55.
20. Wang X, Zhao J, Huang J, Tang H, Yu S, Chen Y. The regulatory roles of miRNA and methylation on oncogene and tumor suppressor gene expression in pancreatic cancer cells. Biochem Biophys Res Commun 2012;425:51–7.

Published OnlineFirst March 27, 2014; DOI: 10.1158/0008-5472.CAN-13-2470

Cancer Research
The Journal of Cancer Research (1916–1930) | The American Journal of Cancer (1931–1940)

AACR American Association for Cancer Research

Biallelic *DICER1* Mutations in Sporadic Pleuropulmonary Blastoma

Masafumi Seki, Kenichi Yoshida, Yuichi Shiraishi, et al.

Cancer Res 2014;74:2742-2749. Published OnlineFirst March 27, 2014.